Cancer Letters 442 (2019) 170–180

Contents lists available at ScienceDirect

Cancer Letters

journal homepage: www.elsevier.com/locate/canlet

Original Articles

NEO212, a conjugate of temozolomide and perillyl alcohol, blocks the endothelial-to-mesenchymal transition in tumor-associated brain endothelial cells in glioblastoma

Nagore I. Marín-Ramos[a], Niyati Jhaveri[a], Thu Zan Thein[a], Rochelle A. Fayngor[a], Thomas C. Chen[a,b], Florence M. Hofman[a,b,*]

[a] Department of Neurosurgery, Keck School of Medicine, University of Southern California, 2011 Zonal Avenue, Los Angeles, CA 90033, USA
[b] Department of Pathology, Keck School of Medicine, University of Southern California, 2011 Zonal Avenue, Los Angeles, CA 90033, USA

ARTICLE INFO

Keywords:
EndMT
Glioma stem cells (GSC)
TGF-β
Notch
Smad

ABSTRACT

As the endothelial-to-mesenchymal transition (EndMT) supports the pro-angiogenic and invasive characteristics of glioblastoma multiforme (GBM), blocking this process would be a promising approach to inhibit tumor progression and recurrence. Here, we demonstrate that glioma stem cells (GSC) induce EndMT in brain endothelial cells (BEC). TGF-β signaling is necessary, but not sufficient to induce this EndMT process. Cell-to-cell contact and the contribution of Notch signaling are also required. NEO212, a conjugate of temozolomide and perillyl alcohol, blocks EndMT induction and reverts the mesenchymal phenotype of tumor-associated BEC (TuBEC) by blocking TGF-β and Notch pathways. Consequently, NEO212 reduces the invasiveness and pro-angiogenic properties associated with TuBEC, without affecting control BEC. Intracranial co-implantation of BEC and GSC in athymic mice showed that EndMT occurs *in vivo*, and can be blocked by NEO212, supporting the potential clinical value of NEO212 for the treatment of GBM.

1. Introduction

Glioblastoma multiforme (GBM) is a highly vascularized brain tumor, exhibiting blood vessels that are disorganized, leaky, dilated and tortuous. Tumor-associated brain endothelial cells (TuBEC) from tumor vasculature are phenotypically and functionally different from control BEC [1–3].

Epithelial-to-mesenchymal transition (EMT) is a reversible process where epithelial cells acquire the phenotypic and functional characteristics of mesenchymal cells [4], and is associated with tumorigenesis and metastasis [5]. A similar process was described for endothelial cells (EC), called endothelial-to-mesenchymal transition (EndMT) [6]. EndMT implies a progressive loss of endothelial markers like CD31 and von Willebrand factor (VWF), and of cell-to-cell adhesion proteins like E-cadherin; and transition towards a mesenchymal phenotype showing high expression of markers like N-cadherin, α-smooth muscle actin (α-SMA) and smooth muscle protein 22-alpha (SM22-α), and increased cell migration and invasion. As EndMT is critical for tumor angiogenesis and progression [7], its blockade would have direct anti-tumor effects.

The changes in morphology and function that occur during the transition from BEC to TuBEC follow a pattern that resembles EndMT. TuBEC are resistant to chemotherapy, including temozolomide (TMZ) [8], and are highly invasive and migratory, characteristics of mesenchymal cells [2]. We hypothesized that EndMT may be involved in the development of tumor vasculature, characterized by increased cell proliferation, migration, vessel permeability and angiogenesis [9].

Our previous results showed that NEO212, a conjugate of TMZ and perillyl alcohol (POH), blocks glioma stem cell (GSC) migration and invasion [10]. As focal adhesion kinase (FAK) is essential for migration and metastasis in cells undergoing EMT or EndMT [5,11], we hypothesized that NEO212 could block this EndMT.

Here we show that NEO212 not only blocks the GSC-induced EndMT in BEC, but also reverts TuBEC from their mesenchymal to a endothelial phenotype, causing a 'mesenchymal-to-endothelial transition' (MEndT). Transforming growth factor-β (TGF-β) is required for EndMT induction, but is not enough to activate this process alone. Secreted factors do not trigger EndMT, as evidenced by conditioned

Abbreviations: EndMT, endothelial-to-mesenchymal transition; GSC, glioma stem cells; TuBEC, tumor-associated brain endothelial cells

* Corresponding author. Departments of Pathology and Neurosurgery, Keck School of Medicine, University of Southern California, 2011 Zonal Avenue, Los Angeles, CA 90033, USA.
E-mail address: hofman@usc.edu (F.M. Hofman).

https://doi.org/10.1016/j.canlet.2018.10.034
Received 18 May 2018; Received in revised form 12 October 2018; Accepted 24 October 2018

media experiments. Cell-to-cell contact and Notch signaling are necessary for a complete EndMT induction. Nevertheless, co-activation of Notch and TGF-β pathways has an additive effect on EndMT induction. NEO212 reduces TGF-β secretion by TuBEC, GSC and GSC + BEC co-cultures, but not by BEC cultured alone. The compound also decreases the activation of the TGF-β downstream effector Smad3. Besides, NEO212 inhibits Notch signaling, and the EndMT induced by DLL1, alone or in combination with TGF-β.

NEO212 reduces the invasiveness of TuBEC, and of BEC co-cultured with GSC. Correspondingly, it decreases the production of matrix metalloproteinases MMP2 and MMP9. Furthermore, NEO212 specifically blocks tubule formation of the abnormal vessels produced by TuBEC, without affecting those derived from BEC. Intracranial co-implantation of BEC and GSC in athymic mice showed that the GSC-driven EndMT in BEC occurs *in vivo*, and is blocked by NEO212.

2. Materials and methods

2.1. Cell isolation

Human tissues were obtained following written informed consent from patients in accordance with Declaration of Helsinki and the Institutional Review Board (HS-09-00520), at Keck School of Medicine, USC. Isolation of cells was described elsewhere [3,12]. Data regarding culture conditions and treatment with inhibitors was included as Supp. Material.

2.2. Protein expression analysis

The detailed protocol for western blot was published [13]. Protein bands were visualized in an ImageQuant LAS4000 (GE Healthcare), and quantified using Image*J* (NIH). Data from three independent experiments were presented.

Immunostaining was performed as previously described [14]. Pictures were taken in an Eclipse 80i microscope (Nikon) or an Olympus BH-2 for biotinylated antibodies, and in a Zeiss LSM 510 confocal microscope (Carl Zeiss Inc.). Images are representative of three-five independent experiments performed in triplicates.

Data regarding antibodies used were included as S. Table 1.

2.3. ELISA

Supernatants were analyzed for TGF-β content using a commercially available ELISA kit (Proteintech). Absorbance was measured in a Fluostar Omega microplate reader (BMG Labtech). Data were normalized to kit controls, and to the number of producing cells. Data from at least three independent experiments in triplicates were presented.

2.4. RNA expression studies

RNA was isolated using the RNeasy Plus Mini Kit (Quiagen). cDNA was obtained with iScript Advanced cDNA Synthesis kit (Bio-Rad). qPCR was performed using the primer sequences indicated in S. Table 2, or the Human Notch Signaling Pathway Plus RT^2 Profiler PCR Array, with SsoAdvanced Universal SYBR Green Supermix (Bio-Rad). Amplifications were run in a StepOnePlus cycler (Applied Biosystems).

2.5. Invasion assays

The protocol was published [10]. Photos were taken in an Eclipse 80i microscope or an Eclipse TE300 Inverted Microscope (Nikon), and cells counted with Image*J*. Data from three independent experiments performed in triplicate were presented.

2.6. Tubule formation assays

Tubule formation was performed as described by Arnaoutova and Kleinman [15]. CalceinAM-labeled cells were photographed with an Eclipse TE300 Inverted Microscope (Nikon). Relative branch/tubule length and number were quantified using Image*J* and the Angiogenesis Analyzer plugin [16]. Data presented were from three independent experiments performed in triplicate.

2.7. In vivo studies

Animal protocols were approved by the USC Institutional Animal Care and Use Committee (IACUC), and strictly adhered to their guidelines. A mixture of 10^5 GSC (USC02) and 3.3×10^4 BEC in PBS was implanted into the subcortical brain parenchyma of 8-week-old female athymic nude mice (Charles River Laboratories). The implantation coordinates were 1.0 mm posterior, 1.0 mm lateral (right) with respect to bregma, and 2.5 mm ventral depth. Implantation volume was 3 μL, and a 24G 5.0 μL glass syringe (Hamilton) was used. Daily treatment started 7 days post-implantation. NEO212 was dissolved in ethanol:glycerol 1:1 with a final DMSO concentration of 5%, and a 100 μL dose of 50 mg/kg or vehicle (5% DMSO in ethanol:glycerol 1:1) were administered subcutaneously. Mice were euthanized 10 or 20 days post-treatment in compliance with USC IACUC's SOP for Rodent Euthanasia. Brains were frozen in VWR Frozen Section Compound for histological analysis.

2.8. Statistical analysis

Statistical analysis was performed using GraphPad Prism 5.0. $P < 0.05$ was considered significant using paired two-tailed *t*-test or 1-way ANOVA followed by Dunnet's multiple comparison test.

3. Results

3.1. Co-culture with GSC induces EndMT in BEC

GSC are closely associated with EC in GBM [17]. A subpopulation of TuBEC displays mesenchymal features like the cytoskeletal marker of mesenchymal cells α-SMA [4], and enhanced migration and invasion [2]. We hypothesized that GSC may be responsible for this transition from BEC to TuBEC. To test this GSC-BEC interaction, we established an *in vitro* co-culture system where patient-derived GSC (USC02 [12]) and BEC were co-cultured for 120 h, then analyzed for α-SMA expression [4]. When cultured separately, GSC and BEC showed few, if any, α-SMA-positive cells. Co-culturing GSC + BEC significantly upregulated α-SMA expression (Fig. 1A). To determine which population was undergoing EndMT, GFP-labeled BEC were co-cultured with GSC. Immunofluorescence analysis demonstrated that α-SMA was expressed by GFP-positive BEC only in co-culture with GSC, and not by GSC, providing evidence that GSC trigger EndMT in BEC (Fig. 1B).

To investigate the kinetics of this process, GSC + BEC co-cultures were fixed at different time-points and immunostained for the endothelial markers endoglin and VWF, and the mesenchymal markers α-SMA and SM22-α. α-SMA and SM22-α expression increased with time of co-culture, suggesting a progressive phenotypic transformation to mesenchymal-like cells. Correspondingly, the expression of the endothelial markers endoglin and VWF decreased in a time-dependent manner, with the positive staining almost gone after 72 h of co-culture (Fig. 1C).

To determine whether EndMT induction is specific to this GSC population or can be caused by other GSC subtypes or non-stem GBM cells, we performed co-cultures of another patient-derived GSC (USC04 [12]), and of U251 cells with BEC. Both USC04 + BEC and U251 + BEC co-cultures exhibited increased α-SMA expression (S.Fig. 1), suggesting that EndMT can be induced by different GSC and non-stem glioma cells.

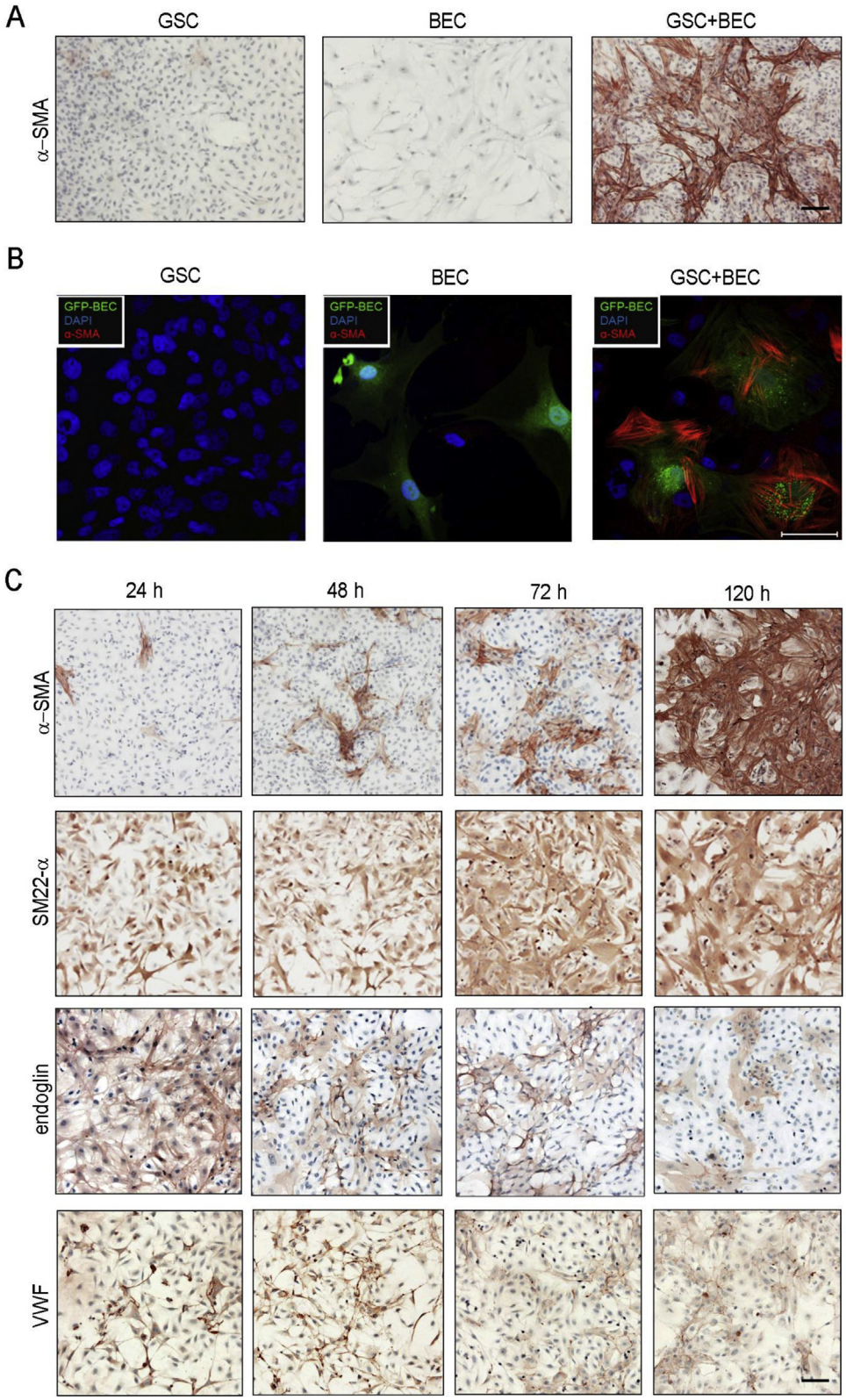

Fig. 1. GSC induce EndMT in BEC in a time-dependent manner. (A) Representative images of α-SMA immunostaining in GSC, BEC and GSC + BEC co-cultures after 120 h. (B) Fluorescence staining for α-SMA (red) in GSC and GFP-BEC cultured alone, and in co-culture, after 120 h. DAPI was used to counterstain all nuclei. (C) Representative images of α-SMA and SM22-α (mesenchymal markers), and endoglin and VWF (endothelial markers) after different co-culture times. Bars, 100 μm. (For interpretation of the references to colour in this figure legend, the reader is referred to the Web version of this article.)

3.2. NEO212 blocks GSC-driven EndMT

Our previous studies showed that NEO212 inhibits tumor progression by reducing GSC migration and invasion [10,12]. As these characteristics are highly related to EndMT, we hypothesized that NEO212 may affect GSC-induced EndMT in BEC. To test this

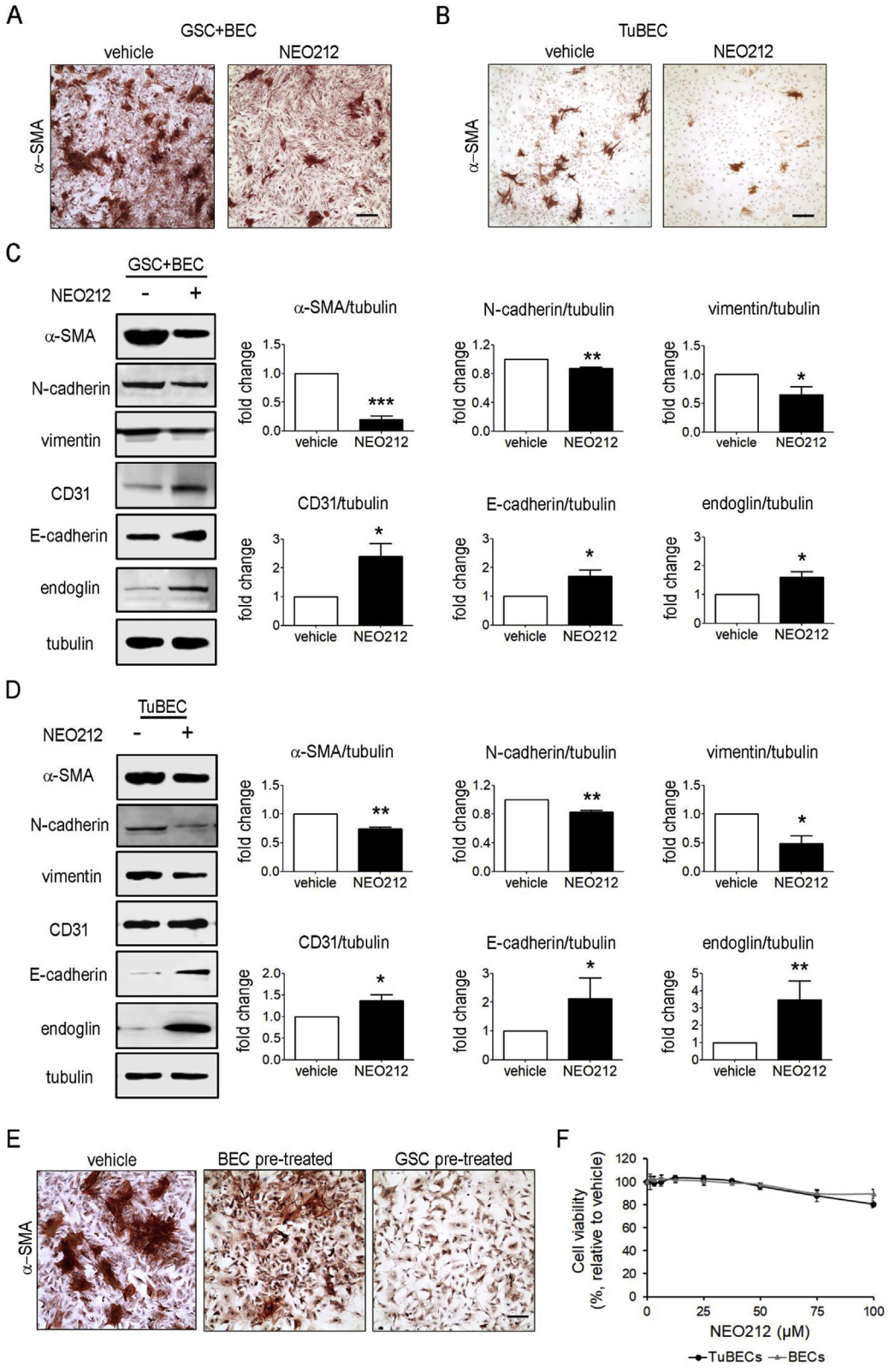

Fig. 2. NEO212 impairs EndMT induction. (A–B) 15 μM NEO212 decreases α-SMA expression in (A) GSC + BEC co-cultures and (B) TuBEC. Bars, 100 μm. (C–D) NEO212 (15 μM) decreases the protein levels of mesenchymal markers (α-SMA, N-cadherin, vimentin) and increases the endothelial markers (CD31, E-cadherin, endoglin) in (C) GSC + BEC co-cultures and (D) TuBEC [n = 3, mean ± SEM. *, $P < 0.05$; **, $P < 0.01$; ***, $P < 0.001$ (relative to vehicle-treated cells)]. (E) NEO212 exerts its effects mainly through GSC. Representative images of α-SMA immunostaining of GSC + BEC co-cultures where cells received no pre-treatment before co-culture (left), BEC were pre-treated with 15 μM NEO212 (middle), or GSC were pre-treated with 15 μM NEO212 before co-culture (right). Bars, 100 μm. (F) NEO212 is not cytotoxic for EC. Graph represents the percentage of cell viability of BEC (grey) or TuBEC (black) relative to vehicle-treated cells.

hypothesis, GSC + BEC co-cultures were treated with 15 μM NEO212, a concentration causing antitumor effects in GSC, with no significant cytotoxicity [10]. α-SMA immunostaining showed a substantial decrease in the number of BEC that undergo EndMT with NEO212 (Fig. 2A). To determine whether NEO212 was only capable of preventing EndMT induction or could also revert the mesenchymal characteristics of TuBEC, we treated TuBEC with NEO212, and observed a decreased α-SMA expression, compared to vehicle-treated cells (Fig. 2B).

We further studied the effects of NEO212 on several classical mesenchymal (α-SMA, N-cadherin, vimentin) and endothelial (CD31, endoglin, E-cadherin) markers. After 72 h-treatment of GSC + BEC co-cultures with NEO212, the protein levels of the mesenchymal markers decreased, while the endothelial markers increased (Fig. 2C). BEC and

GSC cultured separately served as controls. Some of the markers were not expressed in BEC and GSC when cultured individually, and when expressed, NEO212 had no effect (S.Fig. 2). TuBEC treated with NEO212 showed similar changes in their expression pattern to GSC + BEC co-cultures (Fig. 2D), confirming that NEO212 reverts the EndMT.

To test whether NEO212 blocked this GSC-BEC interaction through GSC and/or BEC, we pre-treated these cell populations individually with NEO212 for 72 h, and then co-cultured them with untreated BEC or GSC, respectively. No treatment was added during co-culture. After 72 h-co-culture, in both cases the percentage of positive cells decreased compared to vehicle-treated cells. However, the biggest α-SMA reduction was obtained when GSC were pre-incubated with NEO212 (Fig. 2E), suggesting that it exerts its anti-EndMT effects essentially on GSC.

NEO212 does not significantly affect USC02-GSC viability at 15 μM after 72 h [10,12]. To exclude cytotoxic effects on EC, we performed MTT assays and observed that viability of BEC and TuBEC was not affected by NEO212 at these concentrations, even after 120 h (Fig. 2F). This indicates that NEO212 is specifically blocking the GSC-induced EndMT in BEC, not causing unspecific cytotoxicity.

3.3. TGF-β signaling is necessary but not sufficient to induce EndMT in BEC, and is decreased by NEO212

To elucidate NEO212 mechanism of action to block EndMT, we studied the pathways most likely related to EndMT in EC: TGF-β, Notch, and the downstream transcription factors ZEB, SNAIL and TWIST [18–23].

The role of TGF-β1/β2 in EndMT has been described [24–26]. We treated BEC with different concentrations of TGF-β1 and/or TGF-β2 (1–100 ng/mL), for 24, 48, 72, 96 and 120 h, and immunostained for α-SMA. No differences between vehicle and treatments were assessed (data not shown), although TFG-β treatment effectively caused Smad3 phosphorylation in BEC (S.Fig. 3), suggesting that TGF-β alone is not sufficient to induce EndMT in our patient-derived BEC. To test whether TGF-β has any role in this EndMT, a TGF-βRI/II dual inhibitor, LY2109761 [27], was used. When GSC + BEC co-cultures were treated with 10 μM LY2109761, no α-SMA expression was observed (Fig. 3A). This suggests that, although TGF-β is not the only driving force in EndMT, the activation of this pathway is necessary to induce EndMT in BEC. Western blot analysis showed a significant decrease in mature TGF-β levels only when GSC were treated with NEO212, but not with any of its components, TMZ and/or POH (Fig. 3B). ELISA analysis showed that NEO212 significantly decreased TGF-β secretion by TuBEC, and by GSC alone or in co-culture with BEC, but not by BEC cultures (Fig. 3C). Additionally, NEO212 decreased the phosphorylation of Smad3, a downstream effector TGF-βR [28], in GSC + BEC co-cultures and TuBEC cultures, indicating that NEO212 impairs TGF-β signaling (Fig. 3D).

Bone morphogenetic protein (BMP) signaling occurs in parallel with TGF-β, each one triggering the phosphorylation of a different subset of Smad proteins, and it was related to EndMT [6]. We studied the effects of NEO212 in the phosphorylation of the BMP intracellular effectors Smad1 and Smad5 [29]. There was no difference in their activation levels with NEO212 (Fig. 3D), suggesting that BMP signaling is not likely involved in the EndMT blockade caused by NEO212.

To determine whether other GSC-secreted factors were involved, we tested the effects of conditioned media (CM). CM was collected from GSC and BEC cultured separately, and from GSC + BEC co-cultures, and added to BEC alone at a ratio of 1:1 CM:EC medium. After 96 h-treatment with CM, α-SMA immunostaining showed that CM from GSC, BEC or GSC + BEC cultures do not induce EndMT in BEC (S.Fig. 4A).

To confirm that no secreted factors were involved, GSC were seeded in the upper chamber of a 0.4 μm-pore-size Boyden chamber, and BEC on gelatin-coated coverslips in the bottom chamber. This pore size is small enough to impede cell migration across the membrane. However, GSC and BEC were in close proximity, assuring factor-cell interaction. No positive α-SMA staining was observed in BEC after 96 h (S.Fig. 4B), confirming that soluble factors do not trigger EndMT.

3.4. Notch signaling is required for EndMT induction and is blocked by NEO212

The data presented thus far suggested that GSC-induced EndMT in BEC requires cell-to-cell contact. Since Notch signaling is known to play a role in EMT and EndMT [19,20,30,31], we investigated its potential role in our system. Treatment of BEC with the Notch inhibitor DAPT [32] (10 μM), decreased EndMT induction in GSC + BEC co-cultures, as evidenced by reduced α-SMA staining (Fig. 4A). This suggests that Notch is involved in GSC-mediated EndMT induction.

To determine how NEO212 affects Notch signaling, we studied its effects in the expression pattern of 84 Notch-related genes, in GSC + BEC co-cultures and in TuBEC. Treatment of GSC + BEC co-cultures with NEO212 significantly affected (fold change ≥ 2) the expression of 6 genes: it downregulated WISP1, HOXB4 and the Notch ligands DLL1 and DLL4; and upregulated SCGB1A1 and PTCRA (Fig. 4B). In TuBEC, NEO212 significantly changed the expression pattern of 16 genes: it downregulated H19, HR, UBD, HOXB4, NRARP, LMO2, DLL1, NOTCH4, PSEN2, CBL, and Hes4; and upregulated LOR, AFAP1L2, CDKN1A, HeyL, and DLL3 (Fig. 4C).

Since NEO212 downregulated DLL1 in GSC + BEC and TuBEC, we treated BEC with DLL1 recombinant protein (1 μg/mL) alone or in combination with NEO212, and stained for α-SMA. Treating BEC with DLL1 increased 4-fold the expression of the Notch target gene HES1 (S.Fig. 5) and was sufficient to induce EndMT, effect that was blocked by NEO212 (Fig. 4D). These results confirmed the role of Notch in EndMT, and the mechanism of action of NEO212 through Notch signaling, and namely, the DLL1 ligand.

To test whether TGF-β supported the EndMT triggered by Notch, we performed these experiments in the presence of TFG-β recombinant protein (10 ng/mL). While TGF-β alone was not able to induce EndMT, in combination with DLL1 it triggered a more robust induction than DLL1 alone, suggesting an additive effect of both pathways. NEO212 blocked this stronger EndMT induction caused by co-activation of Notch and TGF-β pathways (Fig. 4D).

Finally, we analyzed the expression levels of the transcriptional regulators related to EndMT and EMT [22,23,33], ZEB1/2, SNAI1 and TWIST, in BEC and U251 glioma cells treated with vehicle or NEO212 (15 μM) for 72 h. We observed no significant changes in BEC, and more relevant but opposite effects of NEO212 in the regulation of ZEB1 and ZEB2 (S.Fig. 6).

3.5. NEO212 impairs invasion and tubule formation of mesenchymal-like cells

EndMT promotes angiogenesis and invasion [7], critical for GBM progression and recurrence. To evaluate the biological relevance of the effects of NEO212 on EndMT, we analyzed how it affected EC invasion and tubule formation.

For invasion studies, EC were seeded in Matrigel-coated 8 μm-pore-size Boyden chambers and treated with vehicle or NEO212 for 16 h. NEO212 significantly decreased the invasiveness of TuBEC, without affecting BEC (Fig. 5A). To analyze this effect in GSC + BEC co-cultures, GFP-labeled BEC were co-seeded with unlabeled GSC. DAPI was used to identify total number of cells. NEO212-treated BEC were less invasive than vehicle-treated cells (Fig. 5B). Our previous studies showed that NEO212 reduces MMP2 and MMP9, enzymes that degrade the extracellular matrix and are critical for cell invasion and metastasis [34]. Here we show that NEO212 also decreases their protein levels in EC (Fig. 5C).

To study potential effects of NEO212 on the pro-angiogenic

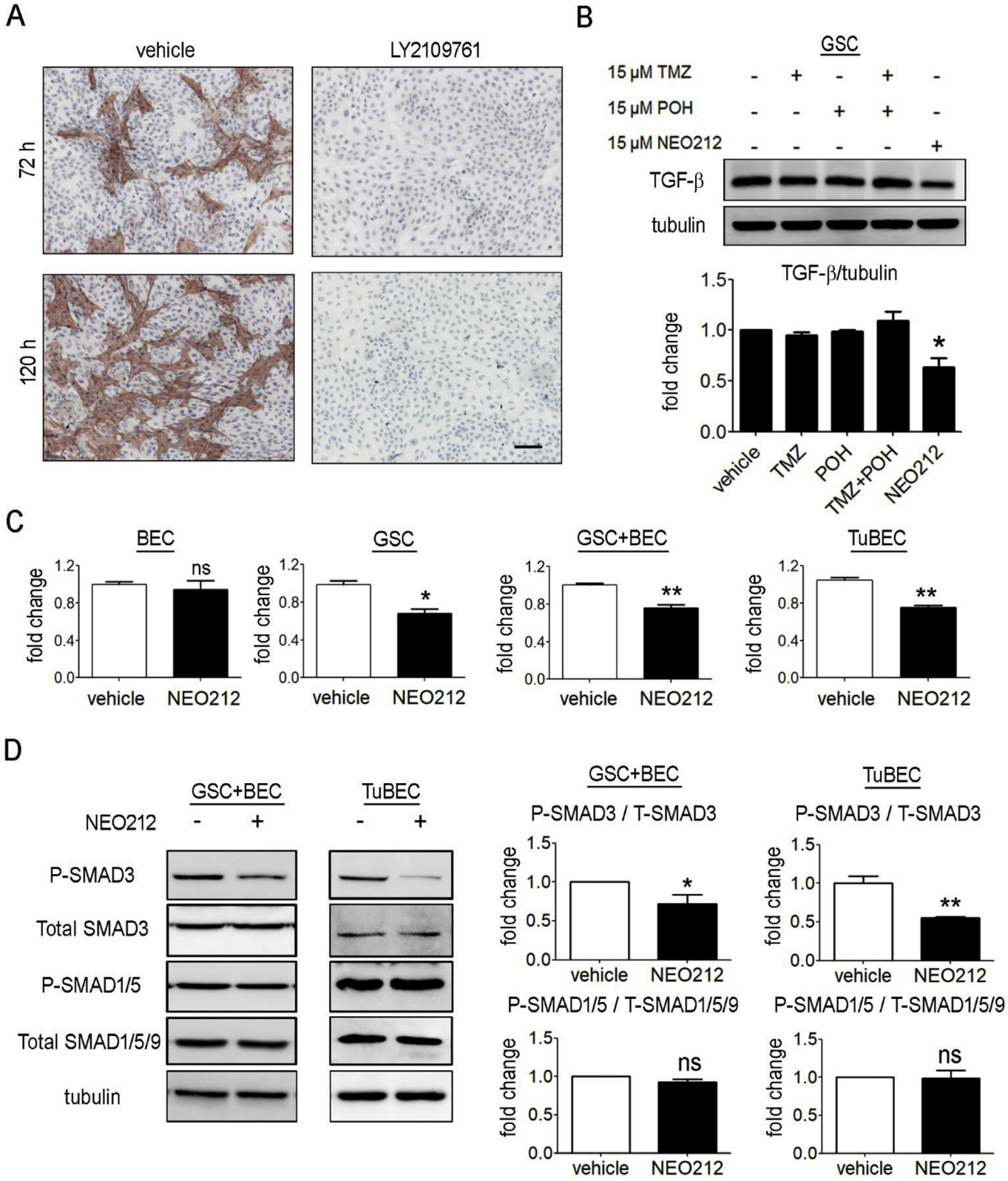

Fig. 3. TGF-β signaling is required but not sufficient to induce EndMT, and is impaired by NEO212. (A) Inhibiting TGF-β signaling blocks the GSC-induced EndMT in BEC. Representative images of α-SMA immunostaining of GSC + BEC co-cultures treated with vehicle or the TGF-βRI/II dual inhibitor LY2109761 for 72 or 120 h. Bars, 100 μm. (B) NEO212 treatment reduces the protein levels of mature TGF-β in GSC, an effect not present with TMZ and/or POH. (C) ELISA analysis of TGF-β secretion by BEC, GSC, GSC + BEC co-cultures and TuBEC, treated with vehicle or 15 μM NEO212. (D) NEO212 reduces the activation of the downstream effector of TGF-β, Smad3, but does not affect the downstream effectors of BMP, Smad1/5. Representative western blots obtained from GSC + BEC co-cultures or TuBEC. In all cases, graphs represent mean ± SEM (n = 3). Ns, not-significant; *, $P < 0.05$; **, $P < 0.01$ (relative to vehicle-treated cells).

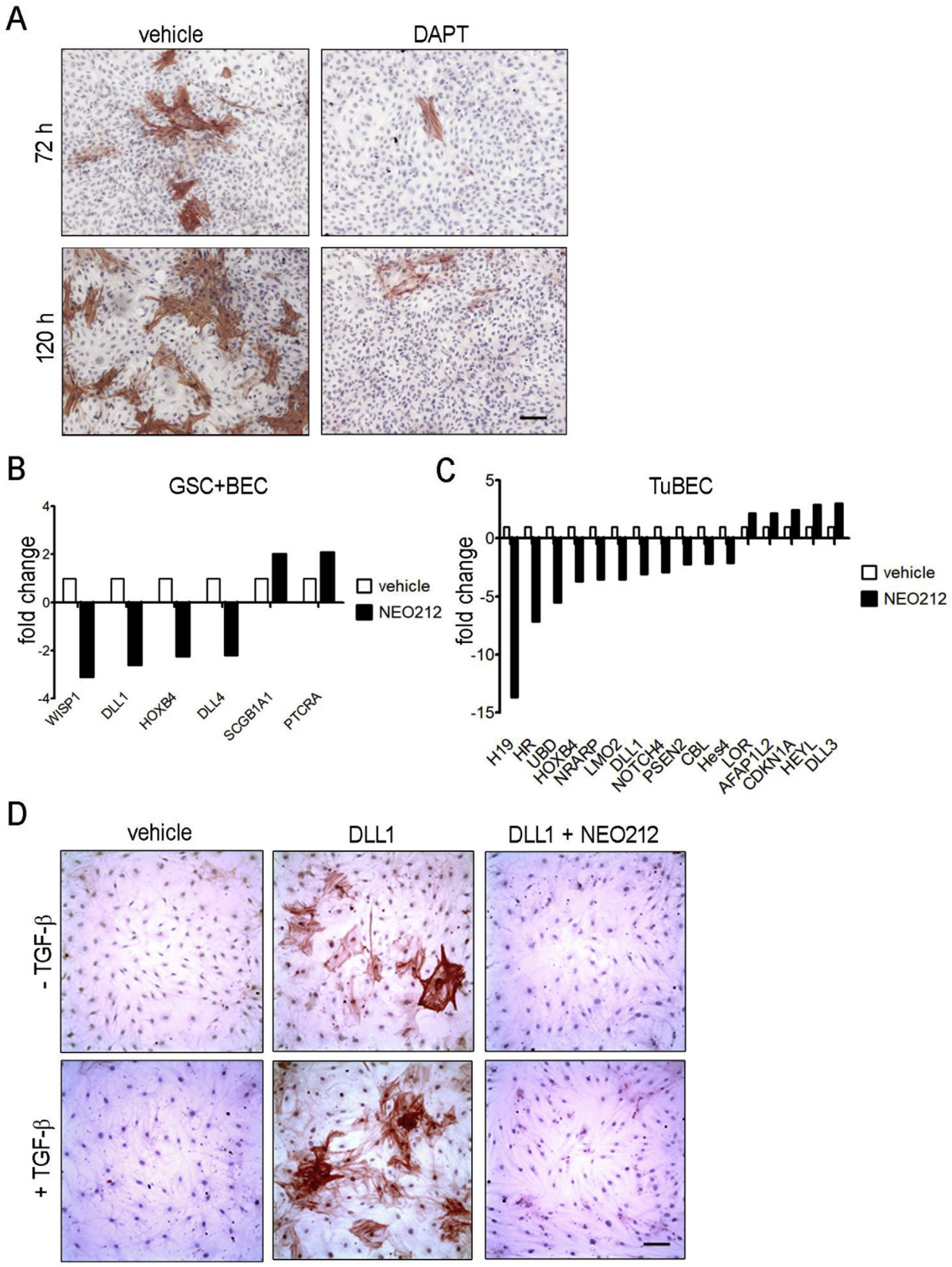

Fig. 4. NEO212 decreases α-SMA expression through inhibition of Notch signaling. (A) Inhibiting Notch signaling blocks the GSC-induced EndMT in BEC. Representative images of α-SMA immunostaining of GSC + BEC co-cultures treated with the Notch inhibitor DAPT. After 72 and 120 h, cells were stained for α-SMA. Bar, 100 μm. (B–C) NEO212 reduces Notch signaling in co-cultures of GSC + BEC and in TuBEC. A Notch signaling PCR array was performed in (B) GSC + BEC co-cultures and (C) cultures of TuBEC. The graphs show the genes regulated by 15 μM NEO212 (threshold = 2-fold change). (D) NEO212 impairs the EndMT induction caused by Notch signaling alone and in combination with TGF-β signaling. Representative images of α-SMA immunostaining of BEC treated with vehicle, DLL1, or DLL1 + 15 μM NEO212, in the absence (upper panels) or presence (lower panels) of TGF-β, for 72 h. Bars, 100 μm.

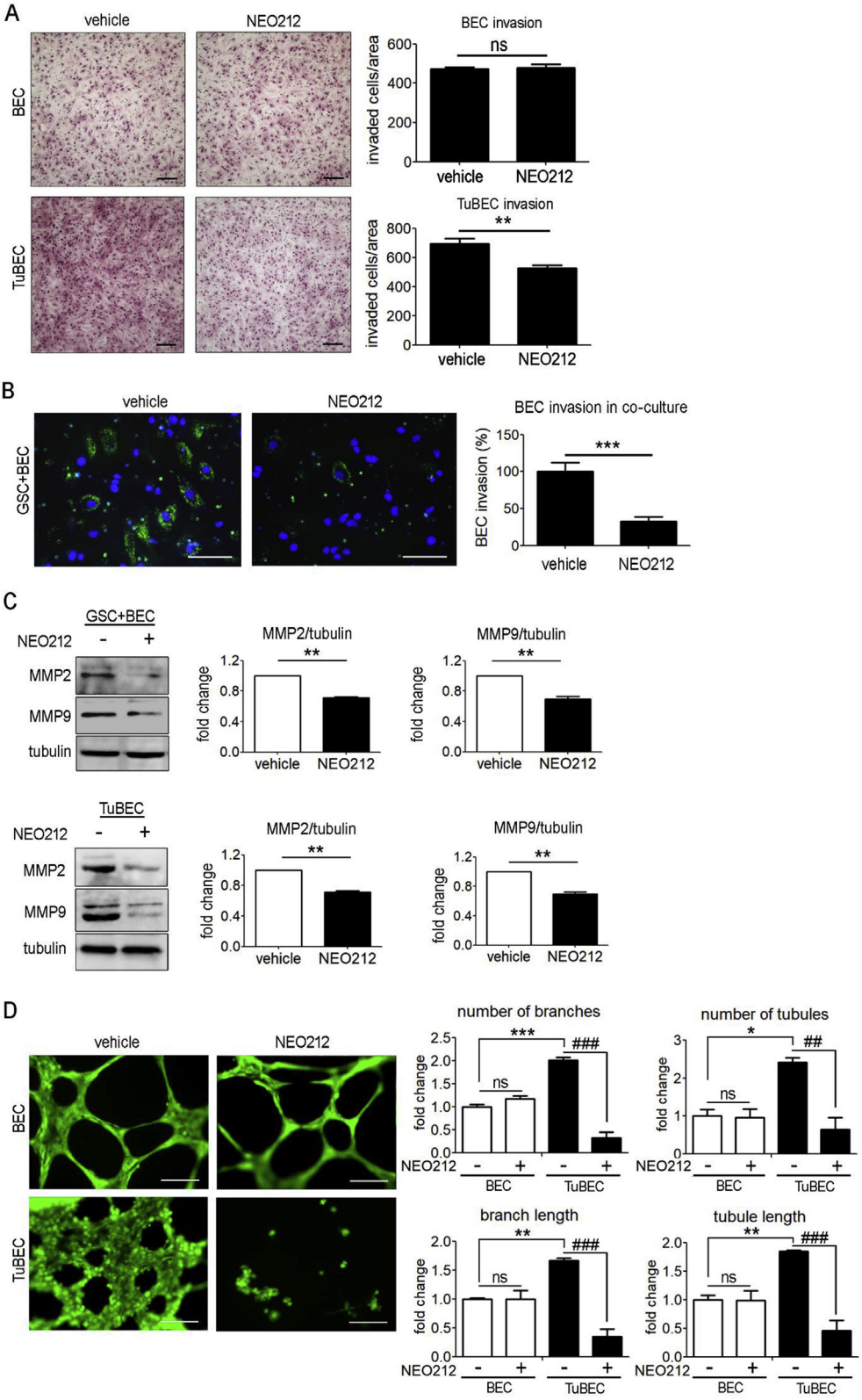

Fig. 5. NEO212 decreases the invasiveness and tubule formation of mesenchymal cells. (A) Representative images of invasion through a Matrigel-coated Boyden Chamber, of BEC and TuBEC cultured alone. Bar, 200 μm. After 16 h-treatments with 15 μM NEO212, the number of invaded cells per field was counted [n = 3 in triplicate, mean ± SEM. Ns, not-significant; **, $P < 0.01$ (relative to vehicle-treated cells)]. (B) Representative images of invasion assay through a Matrigel-coated Boyden chamber, performed with co-cultures of GSC and GFP-BEC [n = 3 in triplicate, mean ± SEM. ***, $P < 0.001$ (relative to vehicle-treated cells)]. DAPI staining was used to detect all nuclei. Bar, 100 μm (C) Western blot analysis of MMP2 and MMP9 in GSC + BEC co-cultures and in TuBEC treated with 15 μM NEO212 or vehicle [n = 3, mean ± SEM. **, $P < 0.01$ (relative to vehicle-treated cells)]. (D) Representative images of tubule formation assay of BEC (upper panels) and TuBEC (lower panels) treated with vehicle or 15 μM NEO212. Bar, 100 μm. Tubule formation assay showed that TuBEC (black bars) exhibit enhanced and aberrant angiogenesis compared with control BEC (white bars). NEO212 selectively impaired tubule formation in TuBEC, decreasing branch and tubule number and length, without affecting BEC [n = 3, mean ± SEM. Ns, not-significant. *, $P < 0.05$; **, $P < 0.01$; ***, $P < 0.001$ (relative to vehicle-treated BEC). ##, $P < 0.01$; ###, $P < 0.001$ (relative to vehicle-treated TuBEC)].

properties of EC, we performed the tubule formation assay with BEC and TuBEC. The tubules formed by TuBEC were thicker, tortuous and abnormal; and NEO212 treatment specifically inhibited the tubule formation of TuBEC, without causing significant changes in BEC (Fig. 5D).

3.6. NEO212 impairs EndMT induction in an in vivo co-implantation GBM model

We demonstrated in an *in vivo* orthotopic glioma model that NEO212 decreased tumor progression by reducing GSC invasion, thereby increasing survival time [10]. To investigate the effects of NEO212 in EndMT *in vivo*, GSC + BEC were co-implanted intracranially

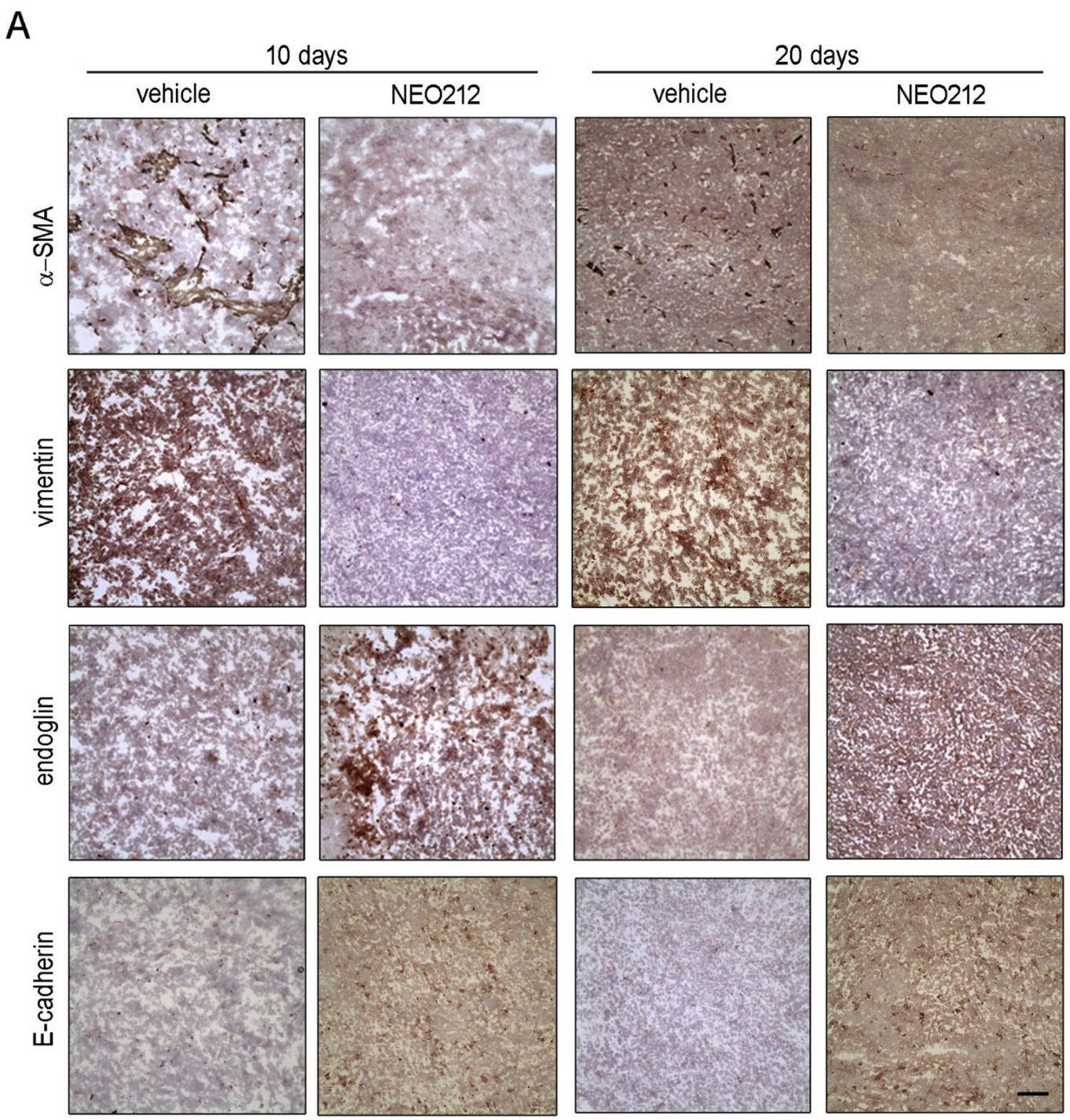

Fig. 6. NEO212 blocks EndMT induction *in vivo*. (A) NEO212 decreases the expression of mesenchymal markers and increases that of the endothelial markers *in vivo*. A mixture of GSC:BEC 3:1 were implanted intracranially in athymic mice. Treatment with 50 mg/kg NEO212 (n = 4) or vehicle (n = 4) was initiated 7 days post-implantation, and mice were euthanized at 10 and 20 days post-treatment. Representative images of brain sections stained for the mesenchymal markers α-SMA and vimentin, and the endothelial markers endoglin and E-cadherin. Bar, 100 μm.

into athymic mice. After euthanization at early (10 days post-treatment) and late (20 days post-treatment) time-points, tumors were analyzed for expression of the mesenchymal markers α-SMA and vimentin, and the endothelial markers endoglin and E-cadherin. NEO212 treatment decreased the mesenchymal markers while the endothelial markers increased, compared to vehicle-treated mice. This effect is observed at the early time-point and is consistent after 20 days of treatment (Fig. 6).

4. Discussion

EndMT occurs in several types of cancer [21,35,36], but we have yet to understand its importance in GBM [1,37]. GSC are associated with vascular niches [17], where EC secrete factors that stimulate GSC self-renewal. There are several studies regarding the effects of the vasculature on CSC and tumorigenesis [1,38], but little is known about how GSC affects the vasculature. Resistance to therapies and tumor recurrence greatly rely on the pro-angiogenic nature and aberrant

vasculature of GBM [39]. Here we examine the dynamic cross-talk between GSC and EC during EndMT. We demonstrate that GSC induce EndMT in BEC (Fig. 1), through a collaboration between TGF-β and Notch pathways (Figs. 3 and 4).

Although GBMs rarely metastasize outside the central nervous system, there is significant infiltration of tumor cells within the brain [40]. Since transformation of cells from endothelial to mesenchymal phenotype supports GBM angiogenesis and invasiveness [1,7], blocking or reverting EndMT would contribute to avoid tumor recurrence. The tumor vasculature is resistant to the standard of care chemotherapy in GBM, TMZ [41]. We show here that NEO212, a conjugate of TMZ and POH, blocks this GSC-induced EndMT by regulating TGF-β and Notch pathways (Figs. 2–4).

TGF-β is not sufficient to trigger EndMT in BEC, but its activation is required, since its blockade by a TGF-βRI/II dual inhibitor impeded the EndMT induction in GSC + BEC co-cultures. Additionally, NEO212 decreased TGF-β levels, and the activation of its downstream effector Smad3 (Fig. 3).

Notch signaling is required for EndMT, as evidenced by the impaired EndMT upon treatment with the Notch inhibitor DAPT. NEO212 downregulated several genes related to Notch, including DLL1, HOXB4, HR, LMO2, NOTCH4, PSEN2 and CBL, as well as Notch target genes, like Hes4 (Fig. 4). In GSC + BEC co-cultures, NEO212 upregulated SCGB1A1, which inhibits the adhesion and migration of EC [42], likely contributing to the decreased BEC invasion in GSC + BEC co-cultures (Fig. 5). In TuBEC, the overexpression of DLL3 caused by NEO212 is important, since it is a Notch antagonist [43]. H19 knockdown with CDKN1A overexpression in HUVEC decreased cell proliferation and capillary-like structures [44]. Hence, the CDKN1A upregulation and H19 downregulation in TuBEC caused by NEO212 may contribute to their impaired tubule formation (Fig. 5D). In both cases, NEO212 downregulated HOXB4 and DLL1 (Fig. 4). Human embryonic stem cells overexpressing HOXB4 differentiate into mesenchymal stem cells [45]. In GBM, DLL1 promotes GSC self-renewal and is expressed in most tumor cells, whereas DLL4 is exclusively expressed in EC. This correlates with our results in the co-culture, where the decrease in DLL1 (expressed in GSC and BEC) is greater than in DLL4 (expressed only in BEC) [46].

To determine whether NEO212 acted through DLL1 downregulation, we treated BEC with vehicle, DLL1, or NEO212 + DLL1; in the absence/presence of TGF-β. DLL1 alone was sufficient to induce EndMT in BEC, although in combination with TGF-β the EndMT induction was stronger, suggesting an additive effect of both pathways. In all cases, NEO212 impaired this EndMT induction. DLL1 did not rescue the EndMT blockade caused by NEO212, suggesting that it not only decreases the expression of DLL1, but also blocks its activity (Fig. 4D).

The transcriptional factors ZEB, SNAI and TWIST are known to be critical for EMT/EndMT induction, especially in the context of hypoxic tumor microenvironments [22,23,33,47]. In GBM, increased cell proliferation, aberrant neovascularization, poor permeability and necrosis can interfere with oxygen perfusion causing hypoxia [33,48]. The increased levels of hypoxia inducible factor 1α (HIF-1α) upregulate ZEB, SNAI, and TWIST expression [22,23,33,49,50], which in turn promote cell invasion, metastasis and EMT/EndMT [51,52]. However, when we treated BEC and U251 glioma cells with NEO212, the levels of SNAI1 and TWIST were minimally altered. Surprisingly, NEO212 caused increased ZEB1 and decreased ZEB2 expression (S.Fig. 6). Although these transcriptional factors are crucial for the EMT/EndMT induction, the lack of overall downregulation suggest that they do not play a major role in the anti-EndMT effects of NEO212.

The biological relevance of this blockade is reflected in the impaired invasiveness of TuBEC, and of BEC in co-culture with GSC, after acquiring mesenchymal features. This correlated with a decrease in MMP2 and MMP9 caused by NEO212. Additionally, the compound specifically blocked the aberrant tubule formation of TUBEC, without affecting BEC (Fig. 5). In the tumor microenvironment, EC are exposed to an amount and number of cytokines and growth factors different from those present in normal brain tissues, which will likely affect receptor expression and signaling pathways. High levels of TGF-β and Notch ligands in gliomas may result in different expression of TGF-β and Notch receptors on TuBEC versus normal BEC [53–56]. This differential regulation of receptor expression due to the microenvironment could explain the selective action of NEO212 on TuBEC versus BEC.

Most GBM preclinical studies use cell lines to model the human disease in mice, which fail to recapitulate many crucial aspects of GBM including invasion and heterogeneity. Most importantly, they fail to consider the critical role of the tumor microenvironment, especially the tumor vasculature. The co-implantation model we use addresses the GSC-BEC interaction, both isolated from human specimens, which increases its clinical significance. This model will be valuable for pan-angiogenesis studies and preclinical screening strategies to better predict clinical response of GBM to novel therapeutics. Here, intracranial co-implantation of GSC + BEC in athymic mice demonstrated that EndMT occurs *in vivo*. NEO212 decreased the expression of mesenchymal markers, and increased the endothelial markers, indicating that it blocks EndMT *in vivo*. This process starts at early point, and remains constant with time of treatment, supporting the clinical value of NEO212 for GBM treatment (Fig. 6). These studies confirm that lower concentrations of NEO212 have effects independent of the cytotoxicity caused by higher doses [10]. This is very unusual in chemotherapy and suggests that lower concentrations of NEO212 may be used for treating other manifestations of GBM, including invasion and EndMT.

Conflicts of interest

T.C. Chen is the CEO/Chairman of, has a commercial research grant from, has ownership interest (including patents), and is a consultant/advisory board member for NeOnc Technologies, Inc. No potential conflicts of interest were disclosed by the other authors.

Acknowledgements/financial support

These studies were supported by NeOnc Technologies, Inc.

Authorship

Experimental design and/or its implementation: N.I. Marín-Ramos, N. Jhaveri, T.Z. Thein, R.A. Fayngor, F.M. Hofman.

Analysis and interpretation of the data: N.I. Marín-Ramos, N. Jhaveri, T.C. Chen, F.M. Hofman.

Writing and revision of the manuscript: N.I. Marín-Ramos, N. Jhaveri, T.Z. Thein, R.A. Fayngor, T.C. Chen, F.M. Hofman.

Appendix A. Supplementary data

Supplementary data to this article can be found online at https://doi.org/10.1016/j.canlet.2018.10.034.

References

[1] N. Jhaveri, T.C. Chen, F.M. Hofman, Tumor vasculature and glioma stem cells: contributions to glioma progression, Cancer Lett. 380 (2016) 545–551.
[2] C. Charalambous, T.C. Chen, F.M. Hofman, Characteristics of tumor-associated endothelial cells derived from glioblastoma multiforme, Neurosurg, Focus 20 (2006) E22.
[3] C. Charalambous, F.M. Hofman, T.C. Chen, Functional and phenotypic differences between glioblastoma multiforme-derived and normal human brain endothelial cells, J. Neurosurg. 102 (2005) 699–705.
[4] R. Kalluri, R.A. Weinberg, The basics of epithelial-mesenchymal transition, J. Clin. Invest. 119 (2009) 1420–1428.
[5] S. Heerboth, G. Housman, M. Leary, M. Longacre, S. Byler, K. Lapinska, A. Willbanks, S. Sarkar, EMT and tumor metastasis, Clin. Transl. Med. 4 (2015) 6.
[6] E. Dejana, K.K. Hirschi, M. Simons, The molecular basis of endothelial cell plasticity, Nat. Commun. 8 (2017) 14361.
[7] S. Potenta, E. Zeisberg, R. Kalluri, The role of endothelial-to-mesenchymal

transition in cancer progression, Br. J. Canc. 99 (2008) 1375–1379.
[8] J.J. Virrey, D. Dong, C. Stiles, J.B. Patterson, L. Pen, M. Ni, A.H. Schonthal, T.C. Chen, F.M. Hofman, A.S. Lee, Stress chaperone GRP78/BiP confers chemoresistance to tumor-associated endothelial cells, Mol. Canc. Res. 6 (2008) 1268–1275.
[9] R.K. Jain, E. di Tomaso, D.G. Duda, J.S. Loeffler, A.G. Sorensen, T.T. Batchelor, Angiogenesis in brain tumours, Nat. Rev. Neurosci. 8 (2007) 610–622.
[10] N.I. Marín-Ramos, T.Z. Thein, H.-Y. Cho, S.D. Swenson, W. Wang, A.H. Schönthal, T.C. Chen, F.M. Hofman, NEO212 inhibits migration and invasion of glioma stem cells, Mol. Canc. Therapeut. 17 (3) (2018) 625–637.
[11] N. Sharma-Walia, K. Patel, K. Chandran, A. Marginean, V. Bottero, N. Kerur, A.G. Paul, COX-2/PGE2: molecular ambassadors of Kaposi's sarcoma-associated herpes virus oncoprotein-v-FLIP, Oncogenesis 1 (2012) e5.
[12] N. Jhaveri, F. Agasse, D. Armstrong, L. Peng, D. Commins, W. Wang, R. Rosenstein-Sisson, V.P. Vaikari, S.V. Santiago, T. Santos, L. Chen, A.H. Schönthal, T.C. Chen, F.M. Hofman, A novel drug conjugate, NEO212, targeting proneural and mesenchymal subtypes of patient-derived glioma cancer stem cells, Cancer Lett. 371 (2016) 240–250.
[13] N.I. Marín-Ramos, D. Alonso, S. Ortega-Gutiérrez, F.J. Ortega-Nogales, M. Balabasquer, H. Vázquez-Villa, C. Andradas, S. Blasco-Benito, E. Pérez-Gómez, Á. Canales, J. Jiménez-Barbero, A. Marquina, J.M. del Prado, C. Sánchez, M. Martín-Fontecha, M.L. López-Rodríguez, New inhibitors of angiogenesis with antitumor activity in vivo, J. Med. Chem. 58 (2015) 3757–3766.
[14] J.J. Virrey, E.B. Golden, W. Sivakumar, W. Wang, L. Pen, A.H. Schönthal, F.M. Hofman, T.C. Chen, Glioma-associated endothelial cells are chemoresistant to temozolomide, J. Neuro Oncol. 95 (2009) 13–22.
[15] I. Arnaoutova, H.K. Kleinman, In vitro angiogenesis: endothelial cell tube formation on gelled basement membrane extract, Nat. Protoc. 5 (2010) 628–635.
[16] M.M.G. Carpentier, J. Courty, I. Cascone, Angiogenesis analyzer for image, J 4th Image J User Dev. Conf, 2012, pp. 198–201.
[17] C. Calabrese, H. Poppleton, M. Kocak, T.L. Hogg, C. Fuller, B. Hamner, E.Y. Oh, M.W. Gaber, D. Finklestein, M. Allen, A. Frank, I.T. Bayazitov, S.S. Zakharenko, A. Gajjar, A. Davidoff, R.J. Gilbertson, A perivascular niche for brain tumor stem cells, Cancer Cell 11 (2007) 69–82.
[18] I.A. Krizbai, Á. Gasparics, P. Nagyőszi, C. Fazakas, J. Molnár, I. Wilhelm, R. Bencs, L. Rosivall, A. Sebe, Endothelial-mesenchymal transition of brain endothelial cells: possible role during metastatic extravasation, PloS One 10 (2015) e0119655.
[19] P. Ghiabi, J. Jiang, J. Pasquier, M. Maleki, N. Abu-Kaoud, N. Halabi, B.S. Guerrouahen, S. Rafii, A. Rafii, Breast cancer cells promote a Notch-dependent mesenchymal phenotype in endothelial cells participating to a pro-tumoral niche, J. Transl. Med. 13 (2015) 27.
[20] C. Sahlgren, M.V. Gustafsson, S. Jin, L. Poellinger, U. Lendahl, Notch signaling mediates hypoxia-induced tumor cell migration and invasion, Proc. Natl. Acad. Sci. Unit. States Am. 105 (2008) 6392–6397.
[21] L. Xiao, D.J. Kim, C.L. Davis, J.V. McCann, J.M. Dunleavey, A. Vanderlinden, N. Xu, S.G. Pattenden, S.V. Frye, X. Xu, M. Onaitis, E. Monaghan-Benson, K. Burridge, A.C. Dudley, Tumor endothelial cells with distinct patterns of TGFβ-driven endothelial-to-mesenchymal transition, Cancer Res. 75 (2015) 1244–1254.
[22] E. Pardali, G. Sanchez-Duffhues, M. Gomez-Puerto, P. ten Dijke, TGF-β-Induced endothelial-mesenchymal transition in fibrotic diseases, Int. J. Mol. Sci. 18 (2017) 2157.
[23] S. Lamouille, J. Xu, R. Derynck, Molecular mechanisms of epithelial–mesenchymal transition, Nat. Rev. Mol. Cell Biol. 15 (2014) 178–196.
[24] E. Arciniegas, A.B. Sutton, T.D. Allen, A.M. Schor, Transforming growth factor beta 1 promotes the differentiation of endothelial cells into smooth muscle-like cells in vitro, J. Cell Sci. 103 (1992) 521–529.
[25] D. Medici, S. Potenta, R. Kalluri, Transforming growth factor-beta2 promotes Snail-mediated endothelial-mesenchymal transition through convergence of Smad-dependent and Smad-independent signalling, Biochem. J. 437 (2011) 515–520.
[26] M.T. Pinto, D.T. Covas, S. Kashima, C.O. Rodrigues, Endothelial mesenchymal transition: comparative analysis of different induction methods, Biol. Proced. Online 18 (2016) 10.
[27] D. Melisi, S. Ishiyama, G.M. Sclabas, J.B. Fleming, Q. Xia, G. Tortora, J.L. Abbruzzese, P.J. Chiao, LY2109761, a novel transforming growth factor beta receptor type I and type II dual inhibitor, as a therapeutic approach to suppressing pancreatic cancer metastasis, Mol. Canc. Therapeut. 7 (2008) 829–840.
[28] Y. Shi, J. Massague, Mechanisms of TGF-beta signaling from cell membrane to the nucleus, Cell 113 (2003) 685–700.
[29] K. Beets, M.W. Staring, N. Criem, E. Maas, N. Schellinx, S.M.C. de Sousa Lopes, L. Umans, A. Zwijsen, BMP-SMAD signalling output is highly regionalized in cardiovascular and lymphatic endothelial networks, BMC Dev. Biol. 16 (2016) 34.
[30] M. Noseda, G. McLean, K. Niessen, L. Chang, I. Pollet, R. Montpetit, R. Shahidi, K. Dorovini-Zis, L. Li, B. Beckstead, R.E. Durand, P.A. Hoodless, A. Karsan, Notch activation results in phenotypic and functional changes consistent with endothelial-to-mesenchymal transformation, Circ. Res. 94 (2004) 910–917.
[31] D. Maciaczyk, D. Picard, L. Zhao, K. Koch, D. Herrera-Rios, G. Li, V. Marquardt, D. Pauck, T. Hoerbelt, W. Zhang, D.M. Ouwens, M. Remke, T. Jiang, H.J. Steiger, J. Maciaczyk, U.D. Kahlert, CBF1 is clinically prognostic and serves as a target to block cellular invasion and chemoresistance of EMT-like glioblastoma cells, Br. J. Canc. 117 (2017) 102–112.
[32] I.-M. Shih, T.-L. Wang, Notch signaling, γ-secretase inhibitors, and cancer therapy, Cancer Res. 67 (2007) 1879–1882.
[33] M. Karsy, J. Guan, R. Jensen, L.E. Huang, H. Colman, The impact of hypoxia and mesenchymal transition on glioblastoma pathogenesis and cancer stem cells regulation, World Neurosurg 88 (2016) 222–236.
[34] K. Komatsu, Y. Nakanishi, N. Nemoto, T. Hori, T. Sawada, M. Kobayashi, Expression and quantitative analysis of matrix metalloproteinase-2 and-9 in human gliomas, Brain Tumor Pathol. 21 (2004) 105–112.
[35] E.M. Zeisberg, S. Potenta, L. Xie, M. Zeisberg, R. Kalluri, Discovery of endothelial to mesenchymal transition as a source for carcinoma-associated fibroblasts, Cancer Res. 67 (2007) 10123–10128.
[36] P.N. Matkar, K. Kumar Singh, D. Rudenko, Y. Jin Kim, M.A. Kuliszewski, G.J. Prud'homme, D.W. Hedley, H. Leong-Poi, Novel regulatory role of neuropilin-1 in endothelial-to-mesenchymal transition and fibrosis in pancreatic ductal adenocarcinoma, Oncotarget 7 (2016) 69489–69506.
[37] M. Huang, T. Liu, P. Ma, R.A. Mitteer, Z. Zhang, H.J. Kim, E. Yeo, D. Zhang, P. Cai, C. Li, L. Zhang, B. Zhao, L. Roccograndi, D.M. O'Rourke, N. Dahmane, Y. Gong, C. Koumenis, Y. Fan, c-Met–mediated endothelial plasticity drives aberrant vascularization and chemoresistance in glioblastoma, J. Clin. Invest. 126 (2016) 1801–1814.
[38] Y. Wang, Y. Wang, H. Chen, Q. Liang, Endothelial cells promote formation of medulloblastoma stem-like cells via Notch pathway activation, J. Mol. Neurosci. 63 (2017) 152–158.
[39] M.E. Hardee, D. Zagzag, Mechanisms of glioma-associated neovascularization, Am. J. Pathol. 181 (2012) 1126–1141.
[40] E.C. Holland, Glioblastoma multiforme: the terminator, Proc. Natl. Acad. Sci. Unit. States Am. 97 (2000) 6242–6244.
[41] C.P. Haar, P. Hebbar, G.C. Wallace, A. Das, W.A. Vandergrift, J.A. Smith, P. Giglio, S.J. Patel, S.K. Ray, N.L. Banik, Drug resistance in glioblastoma: a mini review, Neurochem. Res. 37 (2012) 1192–1200.
[42] G. Antico, M.W. Lingen, A. Sassano, J. Melby, R.W. Welch, S. Fiore, A.L. Pilon, L. Miele, Recombinant human uteroglobin/CC10 inhibits the adhesion and migration of primary human endothelial cells via specific and saturable binding to fibronectin, J. Cell. Physiol. 207 (2006) 553–561.
[43] B. D'Souza, A. Miyamoto, G. Weinmaster, The many facets of Notch ligands, Oncogene 27 (2008) 5148–5167.
[44] C. Voellenkle, J.M. Garcia-Manteiga, S. Pedrotti, A. Perfetti, I. De Toma, D. Da Silva, B. Maimone, S. Greco, P. Fasanaro, P. Creo, G. Zaccagnini, C. Gaetano, F. Martelli, Implication of Long noncoding RNAs in the endothelial cell response to hypoxia revealed by RNA-sequencing, Sci. Rep. 6 (2016) 24141.
[45] Y.-P. Liu, P. Hematti, Generation of mesenchymal stromal cells from a HOXB4-expressing human embryonic stem cells colony, Cytotherapy 11 (2009) 716–725.
[46] T.S. Zhu, M.A. Costello, C.E. Talsma, C.G. Flack, J.G. Crowley, L.L. Hamm, X. He, S.L. Hervey-Jumper, J.A. Heth, K.M. Muraszko, F. DiMeco, A.L. Vescovi, X. Fan, Endothelial cells create a stem cell niche in glioblastoma by providing NOTCH ligands that nurture self-renewal of cancer stem-like cells, Cancer Res. 71 (2011) 6061–6072.
[47] F.A. Siebzehnrubl, D.J. Silver, B. Tugertimur, L.P. Deleyrolle, D. Siebzehnrubl, M.R. Sarkisian, K.G. Devers, A.T. Yachnis, M.D. Kupper, D. Neal, N.H. Nabilsi, M.P. Kladde, O. Suslov, S. Brabletz, T. Brabletz, B.A. Reynolds, D.A. Steindler, The ZEB1 pathway links glioblastoma initiation, invasion and chemoresistance, EMBO Mol. Med. 5 (2013) 1196–1212.
[48] E.E. Bar, A. Lin, V. Mahairaki, W. Matsui, C.G. Eberhart, Hypoxia increases the expression of stem-cell markers and promotes clonogenicity in glioblastoma neurospheres, Am. J. Pathol. 177 (2010) 1491–1502.
[49] W. Zhang, X. Shi, Y. Peng, M. Wu, P. Zhang, R. Xie, Y. Wu, Q. Yan, S. Liu, J. Wang, HIF-1α promotes epithelial-mesenchymal transition and metastasis through direct regulation of ZEB1 in colorectal cancer, PloS One 10 (2015) e0129603.
[50] J.V. Joseph, S. Conroy, K. Pavlov, P. Sontakke, T. Tomar, E. Eggens-Meijer, V. Balasubramaniyan, M. Wagemakers, W.F.A. den Dunnen, F.A.E. Kruyt, Hypoxia enhances migration and invasion in glioblastoma by promoting a mesenchymal shift mediated by the HIF1α–ZEB1 axis, Cancer Lett. 359 (2015) 107–116.
[51] A. Monteiro, R. Hill, G. Pilkington, P. Madureira, The role of hypoxia in glioblastoma invasion, Cells 6 (2017) 45.
[52] I.C. Iser, M.B. Pereira, G. Lenz, M.R. Wink, The epithelial-to-mesenchymal transition-like process in glioblastoma: an updated systematic review and in silico investigation, Med. Res. Rev. 37 (2017) 271–313.
[53] L.-O. Roy, M.-B. Poirier, D. Fortin, Transforming growth factor-beta and its implication in the malignancy of gliomas, Target, Oncol. 10 (2015) 1–14.
[54] B. Kaminska, M. Kocyk, M. Kijewska, TGF beta signaling and its role in glioma pathogenesis, in: J. Barańska (Ed.), Glioma Signaling, Springer Netherlands, Dordrecht, 2013, pp. 171–187.
[55] M.T. Stockhausen, K. Kristoffersen, H.S. Poulsen, The functional role of Notch signaling in human gliomas, Neuro Oncol. 12 (2010) 199–211.
[56] B.W. Purow, R.M. Haque, M.W. Noel, Q. Su, M.J. Burdick, J. Lee, T. Sundaresan, S. Pastorino, J.K. Park, I. Mikolaenko, D. Maric, C.G. Eberhart, H.A. Fine, Expression of notch-1 and its ligands, delta-like-1 and jagged-1, is critical for glioma cell survival and proliferation, Cancer Res. 65 (2005) 2353–2363.